

A Model for the Estimation of the lateral aerodynamic Peak Pressure Load on Cyclists induced by overtaking Vehicles

C. Gromke¹, B. Ruck¹

¹Laboratory of Building and Environmental Aerodynamics, Institute for Hydromechanics, Karlsruhe Institute of Technology KIT, Karlsruhe, Germany, gromke@kit.edu

SUMMARY:

Vehicle-induced aerodynamic loads acting on cyclists in overtaking manoeuvres were measured in full-scale field tests. The test series covered five vehicle types (station wagon, 3.5 t van, 7.5 t truck, tour bus, 40 t semitrailer truck) and four cyclist types being represented by life-size dummies (adult person on touring bike with / without saddle bags, adult person on racing bike, adolescent person on juvenile bike). Time histories of the lateral load were recorded for overtaking manoeuvres at speeds between 30 and 100 km/h and overtaking distances between 0.5 and 2.0 m. The time histories show a rapid increase to a peak pressure load in the early phase of the overtaking manoeuvre. This peak load is also the maximum lateral load which a cyclist experiences during overtaking and is considered a key parameter for cyclist safety. The lateral peak load increases with increasing overtaking speed and decreasing overtaking distance and depends on both vehicle and cyclist type. A model is introduced which allows to calculate the lateral aerodynamic peak pressure load as a function of vehicle type, overtaking speed, cyclist type, and overtaking distance.

Keywords: bicycle aerodynamics, vehicle aerodynamics, traffic-induced flow

1. INTRODUCTION

During overtaking a road vehicle imposes a transient aerodynamic load on a cyclist. The total aerodynamic load can be decomposed into a load acting in driving direction and perpendicular to it. A schematic of the time history of the perpendicular load is illustrated in Fig. 1. The strongest perpendicular (lateral) load F_{peak} occurs in an early phase of the overtaking and is perceived by the cyclist as a lateral pressure load (Gromke and Ruck, 2019).

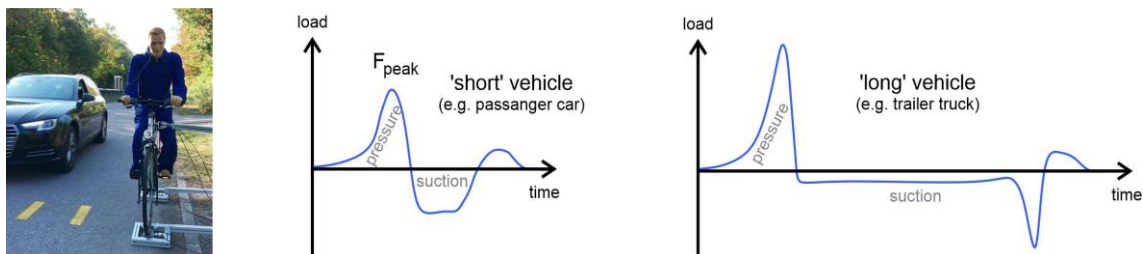


Figure 1. Schematic time histories of lateral load on cyclist in an overtaking manoeuvre.

The peak pressure load F_{peak} is deemed relevant for cyclist safety as immediately upon its occurrence, the strength of the lateral load rapidly decreases and evokes an instantaneous reaction by the cyclist to readjust to the changing equilibrium conditions and to remain in balance.

The current contribution presents a model which allows to estimate the magnitude of the lateral aerodynamic peak pressure load F_{peak} in dependency on the type of the overtaking vehicle, its speed, the cyclist type, and the overtaking distance.

2. METHODS

In a field measurement campaign, time histories of the overtaking vehicle-induced lateral aerodynamic load acting on life-size person dummies on bicycles (dummy-bike assemblies) were acquired. Overtaking manoeuvres were accomplished employing five vehicle types and four dummy-bike assemblies, fixed to a stationary rack using crossbars equipped with load cells (Fig. 2), varying both vehicle speed ($30 \text{ km/h} < V_{\text{veh}} < 100 \text{ km/h}$) and overtaking distance ($0.5 < d_y < 2.0$). The overtaking distance d_y is defined as the spacing between the car envelope - excluding the protruding side mirror - and the central vertical plane of the dummy-bike assembly defined by the bicycle frame.

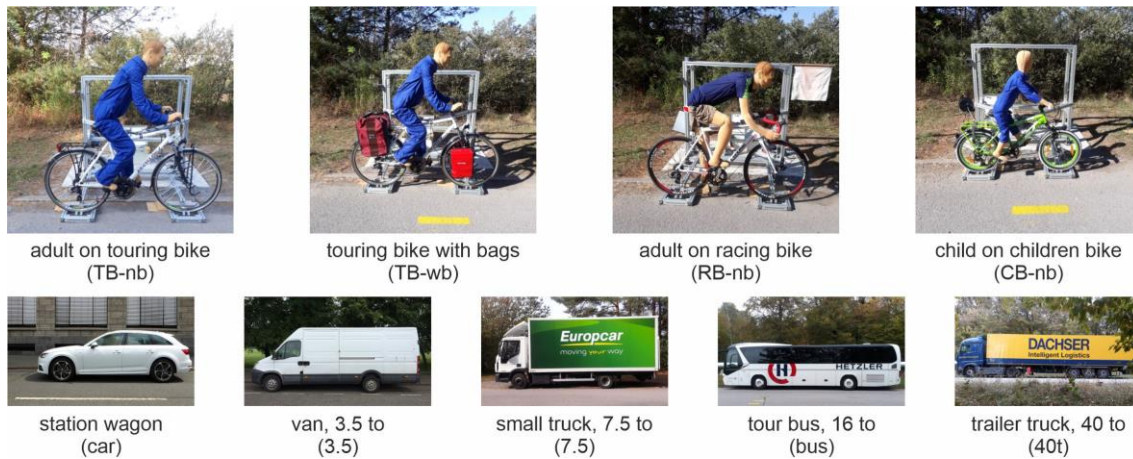


Figure 2. Cyclist types and vehicle types. Terms in brackets are abbreviations to label cyclist and vehicle type.

3. MODEL DEVELOPMENT AND MODEL PERFORMANCE

In a first step of the model development, the lateral aerodynamic peak pressure load F_{peak} obtained from the measurements was fitted by a quadratic relation according to

$$F_{\text{peak}} = c_1 V_{\text{veh}}^2 \quad (1)$$

with V_{veh} the vehicle speed [m/s] and c_1 a pre-factor [kg/m] specific to a cyclist-vehicle type combination at overtaking distance d_y . Fig. 3a shows as an example the measured lateral aerodynamic peak pressure load F_{peak} (symbols) and the fitted curves for the combination of the cyclist on the touring bike without bags (TB-nb) and the passenger car (car).

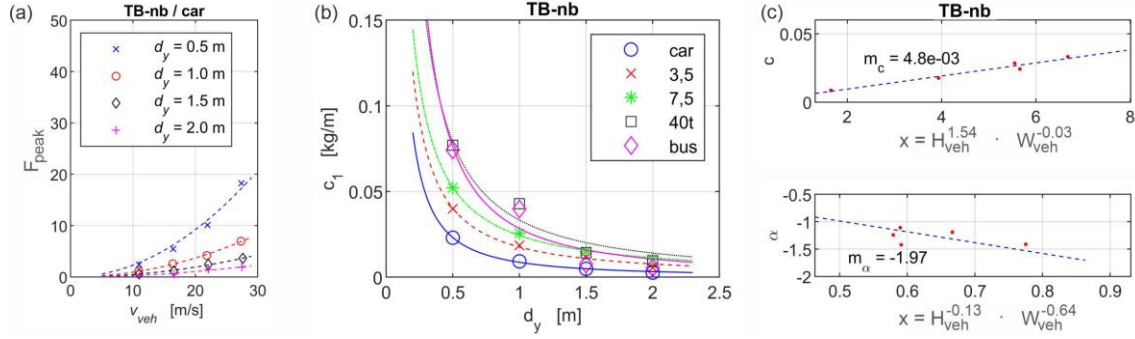


Figure 3. (a) Quadratic curve fits to lateral aerodynamic peak pressure loads F_{peak} accord. to Eq. (1), (b) curve fits to pre-factor c_1 of Eq. (1), (c) curve fits to exponents c and α of Eq. (2) based on Eqs. (3a,b).

The pre-factors c_1 for the cyclist on the touring bike without bags (TB-nb) and all five vehicle types versus the overtaking distance d_y are shown in Fig. 3b. The symbols represent the pre-factors c_1 as obtained from fitting with Eq. (1) and the lines are curve fits obtained with a power function relation according to

$$c_1 = c d_y^\alpha. \quad (2)$$

The form of the functional relationship between the pre-factor c_1 and overtaking distance d_y was inspired by the works of Sanz-Andrés et al., 2003; 2004 and Lichtneger and Ruck, 2015 who studied transient aerodynamic loads induced by vehicles on various nearby objects.

The next step was to determine the pre-factor c and the exponent α of Eq. (2). In this process, it appeared evident to relate both to characteristic geometric dimensions pertaining to the dummy-bike assembly and the vehicle. The key geometric dimensions which largely determine the lateral aerodynamic peak pressure load F_{peak} are the projected frontal area of the vehicle $A_{veh, fro}$ expressed by the product of the vehicle width W_{veh} and height H_{veh} , and the projected lateral area of the cyclist $A_{cyc, lat}$. Hence, in a next step, the values for c and α obtained from curve fits according to Eq. (2) and specific to a certain cyclist type were displayed against products of power functions of H_{veh} and W_{veh} according to

$$c = m_c (H_{veh}^{c_H} \cdot W_{veh}^{c_W}) \quad (3a)$$

$$\alpha = m_\alpha (H_{veh}^{\alpha_H} \cdot W_{veh}^{\alpha_W}). \quad (3b)$$

Based on systematic variations of the exponent pairs c_H & c_W and α_H & α_W and furthermore employing least square fits to the predicted and observed values of c and α according to Eqs. (3a,b) and Eq. (2), respectively, the following best-fit values for the exponents were obtained $c_H = 1.54$, $c_W = -0.03$, $\alpha_H = -0.13$, and $\alpha_W = -0.64$ (valid for all cyclist types). The resulting values for the slope of the linear fit curves were $m_c = 4.1e^{-3}$, $6.4e^{-3}$, $3.6e^{-3}$, $2.9e^{-3}$ and $m_\alpha = -2.35$, -2.08 , -2.27 , -2.23 for the cyclist types TB-nb, TB-wb, RB-nb, and CB-nb, respectively. Fig. 3c presents values of the observed pre-factor c and exponent α (dots) versus predicted linear fit curves (dashed lines) according to Eqs. (3a,b) over abscissae scaled with the best-fit exponent values for the cyclist on the touring bike without bags (TB-nb). It finally remains to relate the

pre-factors m_c and m_α to characteristic geometric dimensions of the dummy-bike assembly and the vehicle. For m_c this was achieved by formulating a linear relation with the cyclist lateral area $A_{cyc,lat}$ according to

$$m_c = m_{c,pf} \cdot A_{cyc,lat} \quad (4a)$$

with $m_{c,pf} = 0.0049$ and for m_α by calculating the mean according to

$$\bar{m}_\alpha = \frac{1}{4} \sum m_\alpha = -2.23. \quad (4b)$$

The combination of Eqs. (1-4) finally provides the mathematical model for the lateral aerodynamic peak pressure load F_{peak} according to

$$F_{peak} = 0.0049 \cdot A_{cyc,lat} \cdot (H_{veh}^{1.54} \cdot W_{veh}^{-0.03}) \cdot d_y^{-2.23} (H_{veh}^{0.13} \cdot W_{veh}^{-0.64}) \cdot V_{veh}^2. \quad (5)$$

Fig. 4 shows for selected combinations of cyclist-vehicle types model-predicted lateral aerodynamic peak pressure loads (lines) and measured loads (symbols). A comparison reveals an overall appropriate performance of the model.

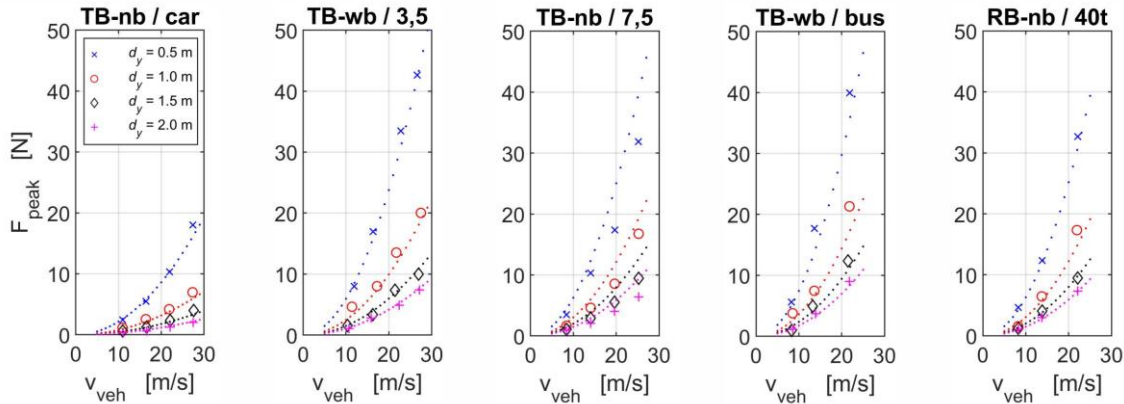


Figure 4. Lateral aerodynamic peak pressure loads F_{peak} for selected combinations of cyclist-vehicle types. Measurement data (symbols) and model-predicted data accord. to Eq. (5) (lines).

ACKNOWLEDGEMENTS

The authors gratefully acknowledge the financial support of the Deutsche Forschungsgemeinschaft DFG (German Research Foundation) under grant Ru 345/32-3.

REFERENCES

- Gromke, C., Ruck, B., 2021. Passenger car-induced lateral aerodynamic loads on cyclists during overtaking. *Journal of Wind Engineering and Industrial Aerodynamics* 209, 104489, 13 pp.
- Lichtneger, P., Ruck, B., 2015. Full scale experiments on vehicle induced transient loads on road-side plates. *Journal of Wind Engineering and Industrial Aerodynamics* 136, 73–81.
- Sanz-Andrés, A., Santiago-Prowald, J., Baker, C., Quinn, A., 2003. Vehicle-induced loads on traffic sign panels. *Journal of Wind Engineering and Industrial Aerodynamics* 91, 925–942.
- Sanz-Andrés, A., Laverón, A., Baker, C., Quinn, A., 2004. Vehicle induced loads on pedestrian barriers. *Journal of Wind Engineering and Industrial Aerodynamics* 92, 413–426.